

Vinh Nguyen¹ and Jeremy Marvel²

Evaluation of Robot Degradation on Human-Robot Collaborative Performance in Manufacturing

Reference

V. Nguyen and J. Marvel, "Evaluation of Robot Degradation on Human-Robot Collaborative Performance in Manufacturing," *Smart and Sustainable Manufacturing Systems* 6, no. 1 (2022): 23–36. <https://doi.org/10.1520/SSMS20210036>

ABSTRACT

Human-robot collaborative systems are highly sought candidates for smart manufacturing applications because of their adaptability and consistency in production tasks. However, manufacturers are still hesitant to adopt these systems because of the lack of metrics regarding the influence of the degradation of collaborative industrial robots on human-robot teaming performance. Hence, this paper defines teaming performance metrics with respect to robot degradation. In addition, the defined metrics are applied to a human-robot collaborative inverse peg-in-hole case study with respect to the degradation of the joint angular encoder and current sensor. Specifically, this case study compares pure insertion versus insertion with spatial scanning to solve the peg-in-hole problem, and manual intervention is implemented in the event of robotic failure. The metrics used in the case study showed that pure insertion more sensitive to robot degradation with manual intervention was required at 0.04° as opposed to 0.12° from insertion with scanning. Therefore, insertion with scanning was shown to be more robust to robot degradation at the cost of a slower insertion time of 9.48 s compared to 3.19 s. Thus, this paper provides knowledge and usable metrics regarding the influence of robot degradation on human-robot collaborative systems in manufacturing applications.

Keywords

manufacturing, degradation, industrial robot, human-robot collaboration

Manuscript received August 2, 2021; accepted for publication November 2, 2021; published online January 13, 2022. Issue published January 13, 2022.

¹ Engineering Laboratory,
Intelligent Systems Division,
National Institute of Standards
and Technology, 100 Bureau Dr.,
Stop 8230, Gaithersburg,
MD 20899-3460, USA
(Corresponding author), e-mail:
vinh.t.nguyen@nist.gov,
 [https://orcid.org/
0000-0003-4617-0892](https://orcid.org/0000-0003-4617-0892)

² Engineering Laboratory,
Intelligent Systems Division,
National Institute of Standards
and Technology, 100 Bureau Dr.,
Stop 8230, Gaithersburg,
MD 20899-3460, USA

Introduction

Smart manufacturing developments in recent years have been characterized by the development of robust yet responsive and flexible systems.¹ Therefore, the adoption of industrial robots as cost-effective and flexible tools toward a variety of manufacturing tasks has been increasing in production facilities in recent years.² However, industrial robots are still limited by their requirements regarding complex end-effector tooling and the inability to compensate for unknown factors arising in the manufacturing environment.³ In addition, human-robot collaborative systems, in which robot(s) work in conjunction with human(s) to accomplish a manufacturing task, are highly appealing in implementing a flexible, efficient, and safe manufacturing environment.⁴ However, manufacturers are still hesitant to adopt human-robot collaborative systems.⁵

One of the reasons that manufacturers are hesitant to adopt such systems is that knowledge of whether a human-robot collaborative system can accomplish a task is limited because of the lack of metrics in the field relative to existing industrial robot metrics.⁶ Thus, prior research regarding human-robot collaboration has been focused on establishing metrics for end users in the manufacturing environment to leverage during the adoption of human-robot collaborative systems. However, metrics in human-robot collaboration in manufacturing have primarily been focused on human safety,^{7,8} communication,^{5,9} and trust^{10,11} with respect to the robot. From a manufacturing viewpoint, an understanding of human-robot systems with respect to how well a task is performed is the key factor when deciding on adoption of human-robot systems. Thus, quantifiable metrics and knowledge of task performance of human-robot systems are critical toward the widespread adoption of human-robot systems in manufacturing environments.

One of the most important influences on manufacturing task performance is structural degradation of equipment. Industrial robots are known to degrade in performance when conducting repeated tasks.¹² Recent research has been conducted toward developing systems focused on detecting robot degradation. For example, Izagirre et al.¹³ demonstrated a vision system using machine learning models to identify degradation in robot positional trajectory performance. Also, Algburi and Gao¹⁴ analyzed robot encoder signals to determine the occurrence of faults in industrial robots. In addition, Weiss and Kaplan¹⁵ demonstrated a detection system where a precision key is inserted into a position-verification sensor to detect robot degradation beyond an acceptable amount. However, prior literature regarding robot degradation is focused on single-robot performance without studying the influence of human-robot interaction.

Thus, this paper has established that the study of the effects of robot degradation on human-robot collaborative systems is limited. Because this knowledge is vital for manufacturers to understand whether human-robot collaborative systems can satisfy their application for long-term manufacturing applications, the lack of such information is a limitation for manufacturers to adopt these systems. Hence, this paper aims to study the influence of robot degradation on the manufacturing performance of human-robot collaborative systems using a case study. In addition, this research aims to establish metrics to consider when deciding among system integrators and robot manufacturers for applications regarding human-robot collaboration. The structure of the paper is as follows. The section titled “Metrics” establishes metrics with respect to robot degradation in human-robot collaboration applications. The “Case Study: Peg-in-Hole” section discusses a peg-in-hole case study with respect to some of the proposed metrics using the behavior of human performance. In addition, a framework for evaluation of the metrics is demonstrated by using two different insertion methods in the “Case Study: Peg-in-Hole” section. The results regarding the influence of robot degradation on robot-human teaming performance are discussed in the “Results” section, which is followed by a “Conclusions” section.

Metrics

This section describes recommended metrics for evaluating robot degradation with respect to human-robot collaborative applications. The metrics in this section are not exhaustive; however, they are critical factors that

production end users and integrators should consider when implementing these systems. Thus, while the case study in this paper examines some of the described metrics, the discussion in this section can still be used to facilitate thoughtful consideration of degradation by end users and system integrators.

ROBOT PERFORMANCE

Many metrics and standards exist with respect to performance of industrial robots including positional accuracy¹⁶ and safety.¹⁷ However, metrics regarding robot degradation are limited, especially considering that robots are subject to thousands of service hours. Thus, this paper recommends consideration of at least the following outlined factors regarding robot degradation, even without the context of human-robot collaborative systems, for completeness.

- **Hardware degradation:** The fundamental sources of robot degradation are because of specific hardware components such as the encoders, motors, and current sensors. Note that while individual components can be evaluated in the context of degradation, how these components interact with each other to contribute to overall degradation in a complex robotic system is not well understood. In addition, most research regarding fault detection of robot degradation monitors the resulting end-application performance as opposed to the fundamental source of degradation. For instance, the position verification sensor demonstrated by Weiss and Kaplan¹⁵ detected faults by evaluating end-effector accuracy resulting from joint degradation as opposed to studying degradation in the joint itself. Hence, understanding the end-application performance deterioration with respect to the fundamental sources of robot errors is vital to diagnostics and degradation mitigation.
- **Robot task performance:** Industrial robots are adopted for a specific task depending on the end-effector tooling and manufacturing environment. Thus, task performance of the robotic system must be quantified as the robot degrades. This includes considering locations along the kinematic chain where sources are the most sensitive to degradation.¹⁸ Thus, while the robot manufacturers can quantify degradation of specific robot components, system integrators must consider degradation of both the tooling and the influence of degrading robot components on positional accuracy.
- **Safety:** While safety standards exist in the current literature, the influence of robot degradation on safety has not been well documented. For instance, force-limiting collaborative robots utilize current sensors to indirectly calculate force, which is compared to a predetermined threshold.¹⁹ Thus, as the quality of current sensors degrades, the force-limiting readings are subject to poor performance, which impacts safety. In addition, while expected to be minor, degradation in the joint encoders can influence the workspace of the robot, which thus impacts the establishment of safe work areas.
- **Servicing:** Note that a robotic system will naturally degrade as part of its operating lifetime. Thus, metrics regarding maintenance, such as frequency of servicing and service downtime, must be quantified for end users to have a full understanding of expenses regarding adopting robotic systems.

PERSONNEL PERFORMANCE

Note that quantifying human performance is subject to variability and subjectivity and is therefore difficult for both robot manufacturers and system integrators to report. However, metrics regarding human performance as the robot degrades are still important for end users to monitor for diagnostics and staffing scheduling. In addition, while metrics regarding social interaction, including trust and communication, are vital to overall human performance, the influence of these metrics on manufacturing performance is still not well understood and is therefore not included with respect to degradation in this work.

- **Effort:** As the robot degrades in a human-robot collaborative system, the human operator must compensate for the robot's performance. Thus, the human would exert more effort to accomplish the collaborative task. Human effort is task-dependent and can be quantified in certain cases such as exerted force in assistive lifting or the number of human interventions after the robot fails a task.
- **Completion time:** In specific cases where robots and humans will conduct tasks sequentially, the human's completion time will be influenced by the robot's performance. Therefore, a robot with degrading

performance will result in a longer completion time by the human, which can therefore contribute to fatigue and overall teaming performance degradation.

- Overall teaming performance: Note that in some applications, the overall teaming performance provides the most relevant metrics for end users. Overall teaming performance metrics include final insertion time and surface finish for collaborative applications as possible examples. However, the aforementioned metrics should still be considered for diagnostics and for providing a holistic interpretation of the process quality.

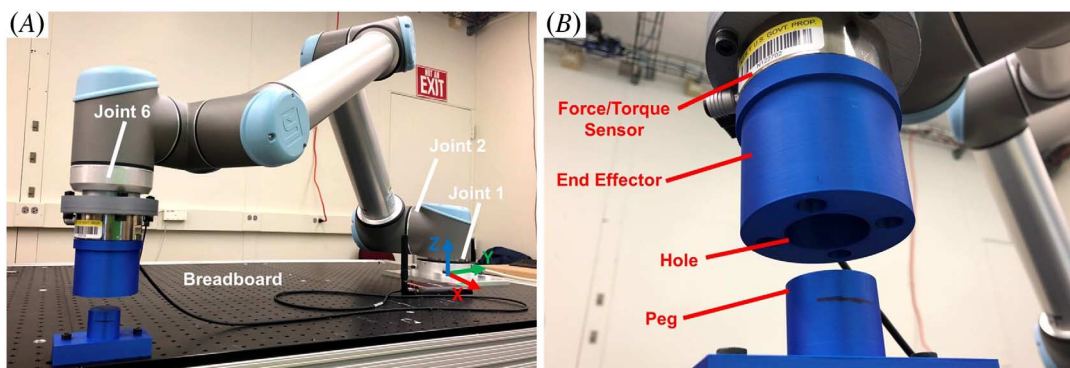
Case Study: Peg-in-Hole

To examine and quantify the influence of robot degradation on human-robot collaboration, a peg-in-hole application setup was implemented at the National Institute of Standards and Technology (NIST). **Figure 1** shows the experimental setup used in this paper. In this work, an end effector with a hole axis perpendicular to the robot flange was mounted onto a UR10 robot with a repeatability of ± 0.1 mm. The goal of the application is to insert the end effector (34.69 mm diameter) onto a peg (34.42 mm diameter), as shown in **figure 1**, with both the robot and the peg mounted onto a 900-mm \times 1,800-mm breadboard. Thus, the case study is represented as a reverse peg-in-hole problem where the hole is mounted onto the robot. This problem is seen in applications including robotic riveting²⁰ and vacuum-based gripping.²¹ Specifically, this is a human-robot collaborative system because the operator initially monitors the robot and then corrects for robot's errors as it is handled by the operator in force-compliance mode. Hence, this specific case study is of interest to the manufacturing community in addition to studying how robot degradation influences human-robot collaboration teaming performance. Initial hole localization is conducted in the X-Y plane, while the insertion motion is performed along the Z axis. If the robot fails to insert the end effector onto the peg because of degradation in its performance, then manual insertion is required to account for the robot performance failure. Thus, this problem represents a sequential manufacturing task where human intervention is required to compensate for robot failures owing to degradation. In this work, two sources of robot degradation are modeled: joint encoder slip in joint 1 and current sensor drift in joint 2.

POSE SELECTION USING SENSITIVITY ANALYSIS

Note that the robot task performance for this case study, identified as the ability to accurately locate the hole based on the initial Cartesian position, is pose-dependent. Therefore, determining the appropriate workspace location is critical for establishing benchmarks to examine the overall task performance. To determine the sensitivity of the robot with respect to degradation in joint 1, consider the following robot kinematic Jacobian for a six-degrees-of-freedom robot.²² Note that this work studies the degradation of joint 1 to avoid misinterpretation of the results stemming from the confounding of the degradation of multiple joints.

FIG. 1 (A) Isometric and (B) detailed views of experimental setup for peg-in-hole case study.



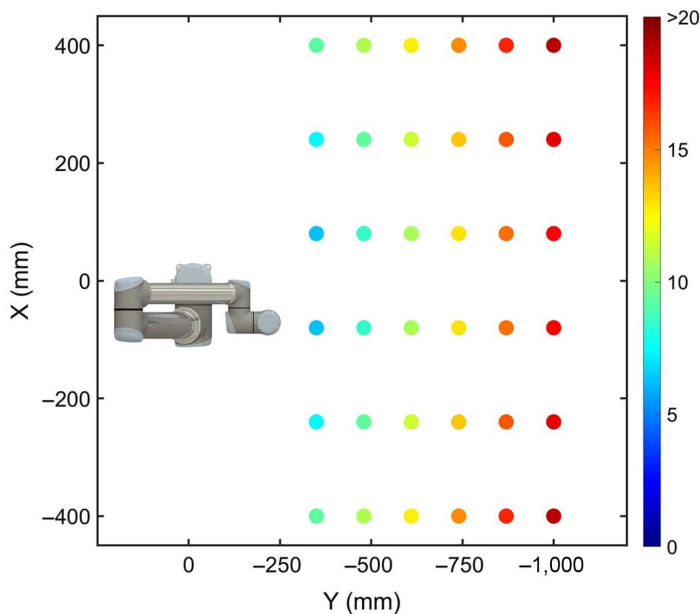
$$J = \begin{bmatrix} \frac{\partial x}{\partial q_1} & \frac{\partial x}{\partial q_2} & \frac{\partial x}{\partial q_3} & \frac{\partial x}{\partial q_4} & \frac{\partial x}{\partial q_5} & \frac{\partial x}{\partial q_6} \\ \frac{\partial y}{\partial q_1} & \frac{\partial y}{\partial q_2} & \frac{\partial y}{\partial q_3} & \frac{\partial y}{\partial q_4} & \frac{\partial y}{\partial q_5} & \frac{\partial y}{\partial q_6} \\ \frac{\partial z}{\partial q_1} & \frac{\partial z}{\partial q_2} & \frac{\partial z}{\partial q_3} & \frac{\partial z}{\partial q_4} & \frac{\partial z}{\partial q_5} & \frac{\partial z}{\partial q_6} \\ \frac{\partial \omega_x}{\partial q_1} & \frac{\partial \omega_x}{\partial q_2} & \frac{\partial \omega_x}{\partial q_3} & \frac{\partial \omega_x}{\partial q_4} & \frac{\partial \omega_x}{\partial q_5} & \frac{\partial \omega_x}{\partial q_6} \\ \frac{\partial \omega_y}{\partial q_1} & \frac{\partial \omega_y}{\partial q_2} & \frac{\partial \omega_y}{\partial q_3} & \frac{\partial \omega_y}{\partial q_4} & \frac{\partial \omega_y}{\partial q_5} & \frac{\partial \omega_y}{\partial q_6} \\ \frac{\partial \omega_z}{\partial q_1} & \frac{\partial \omega_z}{\partial q_2} & \frac{\partial \omega_z}{\partial q_3} & \frac{\partial \omega_z}{\partial q_4} & \frac{\partial \omega_z}{\partial q_5} & \frac{\partial \omega_z}{\partial q_6} \end{bmatrix} \quad (1)$$

where ω_x , ω_y , and ω_z are the rotations about the X, Y, and Z axes, respectively, and q_i is the angular position of the i th joint. Thus, the individual elements of the Jacobian matrix are the sensitivity of an element of the Cartesian position to a specific joint. The individual equations for the Cartesian position (x , y , z , ω_x , ω_y , and ω_z) are obtained from standard forward kinematics using the Denavit-Hartenberg parameters.²³ In this research, the sensitivity of the robot position in the X-Y plane with respect to degradation in joint 1 was studied, so $\frac{\partial x}{\partial q_1}$ and $\frac{\partial y}{\partial q_1}$ were computed by taking the corresponding partial derivatives of the forward kinematics solution for x and y , respectively. This analysis was computed for discrete poses in the X-Y plane 175 mm above the top face of the breadboard shown in **figure 1**. The tool axis was constrained to be perpendicular to the breadboard surface. In addition, because $\frac{\partial \omega_z}{\partial q_1}$ is 0, a fixed ω_z orientation was considered at each discrete point. **Figure 2** shows the vector norm of $\frac{\partial x}{\partial q_1}$ and $\frac{\partial y}{\partial q_1}$ in multiple positions in the robot workspace.

Figure 2 shows that as the arm extends out from its base in both the X and Y directions, the Cartesian position sensitivity with respect to joint 1 increases. This is because as the UR10 end effector extends from its base, the arc distance traveled by the end effector corresponding to a change in joint 1 increases. Therefore, the robot is the most sensitive to degradation in joint 1 at the farthest distance from the robot base. In the workspace poses shown in **figure 2**, the largest sensitivity of 18.8 mm/deg corresponds to X and Y coordinates of ± 400 mm and $-1,000$ mm, respectively. Thus, a minor degradation of 0.01 degrees would result in 0.188 mm of positional error, which can be unacceptable for applications including peg/shaft assembly²⁴ and

FIG. 2

Mapping of X-Y position norm sensitivity to joint 1 (mm/deg). The X-Y coordinates denote the tool axis location. A top view of the UR10 (not to scale) is overlaid for reference.



machining.²⁵ Note that the workspace poses with the lowest sensitivity (X and Y coordinates of ± 80 mm and -350 mm, respectively) exhibit sensitivities of 6.27 mm/deg. Thus, **figure 2** shows that the sensitivity of positional accuracy to joint 1 degradation can change by at least three times based on arm position, and careful selection of where to conduct the analysis is critical.

Force-limiting robots, including the UR10, have been known to utilize current sensors to indirectly calculate force and torques at the robot end effector and joints, respectively. Thus, as the current sensors in the robot degrade, the performance and safety of the robot will suffer as a result. In this case study, degradation in the current sensors in the joint would influence the insertion force threshold. To determine the sensitivity of the force and torque computed by the UR10 at the end effector on the current sensors, the robot was driven to each of the poses shown in **figure 2**. At each position, 10 current and force/torque readings were recorded from the robot controller using the user datagram protocol communication interface. A best fit line of the following form was fitted to the Z-direction force as a function of the current in each joint.

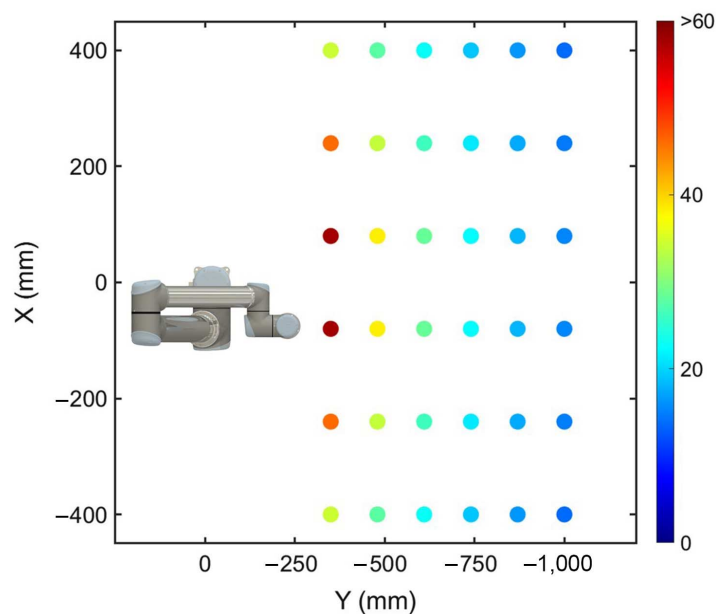
$$F_z = \beta + \sum_{i=1}^6 \alpha_i I_i \quad (2)$$

where β , α_i , and I_i are the intercept, sensitivity coefficient, and current of the i th joint at a given position, respectively. Note that the average R^2 coefficient was 1.0, which indicates that the UR10 also uses linear polynomials to compute force/torque from current readings. In addition, note that α_i is in units of Newton/Ampere and therefore represents the sensitivity of the force component to each individual current sensor. In this work, the influence of the current sensor in joint 2 was considered because it exhibited the highest sensitivity on the Z direction force. Thus, **figure 3** shows the value of α_2 at each position in the workspace.

Note that **figure 3** seems to show opposite trends to those of **figure 2**. Specifically, the end-effector force sensitivity decreases as the robot extends from its base. The lowest sensitivity appears to be at the X and Y coordinates of ± 400 mm and $-1,000$ mm, respectively, while the largest sensitivity corresponds to the X and Y coordinates of ± 80 mm and -350 mm, respectively. This is because as the arm is closer to its base,

FIG. 3

Mapping of absolute Z direction force sensitivity to current sensor in joint 2 (Newton/Ampere). The X-Y coordinates denote the tool-axis location. A top view of the UR10 (not to scale) is overlaid for reference.



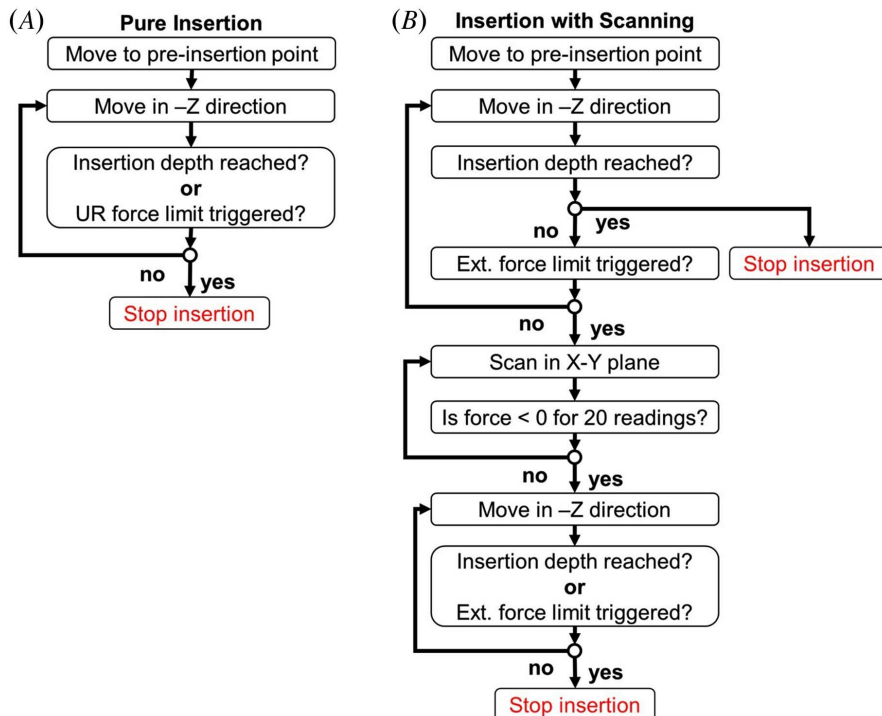
the link attached to joint 2 becomes more collinear with the gravity vector. Thus, perturbations would introduce torque, and therefore, current readings about joint 2 increase as a result. In addition, **figure 3** shows that the smallest and largest sensitivities are 13.8 N/A and 57.7 N/A, respectively.

Even though the force sensitivity is inversely related to the position sensitivity, in this paper the position most sensitive to position degradation was chosen because position sensitivity contributes more directly to the task performance. Specifically, the X and Y coordinates of the peg for the case study were chosen to be 400 mm and -1,000 mm, respectively. Note that this section clearly shows that selection of the robot pose for evaluating metrics is critical for robot degradation and accuracy in general. In addition, this paper demonstrates both modeling and empirical methodologies for selecting the appropriate robot position for metrics evaluation.

METHOD 1: PURE INSERTION

The first method for solving the peg-in-hole problem represents a case where the robot manufacturer only uses positional and force sensors native to the robot. In this procedure, the robot initially drives to the X and Y coordinates directly above the peg. The Z height of the bottom face of the tool is then driven to 2.92 mm above the top face of the peg. The robot then traverses in the Z direction at a speed of 3 mm/s. The insertion stops when either the robot passes 10 mm of insertion or the force in the Z direction passes above 50 N based on the robot end-effector readings. The force limit is set to prevent breakage or significant interference between the mating parts. The force measurements are calculated from current sensors read by the native robot controller. If the robot halts its Z direction traversal after 10 mm of insertion, then the procedure is deemed successful. Otherwise, if the robot stops before 10 mm of insertion, then the procedure is deemed unsuccessful. In the case of an unsuccessful insertion, the human operator manually finishes the insertion by operating the robot in feed-drive mode and manually inserting the tool over the peg. **Figure 4A** shows a flow chart representing the insertion procedure.

FIG. 4 Flow chart of insertion via (A) pure insertion and (B) insertion with scanning methods.



METHOD 2: INSERTION WITH SCANNING

This method initially starts similarly to the previously described pure insertion method. However, if the insertion fails, the robotic system then attempts to scan for the peg location. During this time, the tool is kept in constant contact in the Z direction by using a force controller while the robot moves the end effector in the X-Y plane to search for the peg. The robot uses force measurements in the Z direction to determine when the end effector is placed directly over the peg, and then insertion in the Z direction occurs similarly to the pure insertion method. Note that the UR10 current sensors cannot isolate internal forces (such as forces required to move the end effector) from external forces acting on the end effector. Therefore, an external force sensor is used in this method. Hence, this method is expected to be more expensive and slower than not using an external sensor while being more robust to robot-degradation effects.

Scanning in the X-Y Plane

Note that the UR10 used in this work does not natively support commanding both a point and an end velocity in the decomposed Cartesian directions. However, the UR10 does allow for commanding of velocities in each of the Cartesian directions. Therefore, to enable continuous motion in the X-Y plane, a velocity controller was utilized. Specifically, a unit vector is calculated between the current robot pose and desired position. A commanded velocity scalar value is then projected onto the unit vector, and the resulting vector is commanded to the X and Y Cartesian velocities of the robot. A velocity command is sent to the UR10 every 100 ms. When the robot has reached the waypoint, the next waypoint is set as a reference to the velocity controller. However, note that the robot pose measurements are subject to noise and the robot can pass over the waypoint between sampling times. Therefore, the robot is considered to reach the waypoint when the pose is within a specified radius about the waypoint. The radius of the sphere is calculated as the product of the speed, sampling period, and safety factor, which have values that were set to 1 mm/s, 100 ms, and 0.75, respectively. Note that as the commanded speed increases, the threshold increases. Thus, using this velocity controller method results in a larger positional error as the commanded velocity increases. This behavior coincides with previously established trajectory- and velocity-based controllers.²⁶

Multiple scanning trajectories have been previously demonstrated to solve the peg-in-hole problem such as random, spiral, and raster searches.²⁷ However, spiral searches are difficult to implement with the described velocity controller because the initial small radii of curvature at the beginning of the spiral trajectory result in premature triggering of the waypoint thresholds. In addition, the zero-radius curvature turns in raster searches resulted in sudden accelerations that were found to interfere with the force control in the Z direction. Thus, in this work, scans in the X-Y plane were conducted along a sequence of circles with gradually increasing radii. The radii of the circles were incremented by 0.5-mm up to 2-mm radius. In addition, the arc length spacing of the waypoints along the circle was calculated to be 0.1 mm. Using this approach, a comprehensive search area can be defined while ensuring smooth trajectories along the scanning path.

Force Control in Z Direction

During the scanning period, a constant force was maintained between the end effector and the peg surface using a force controller. In this work, an ATI gamma force/torque sensor with a resolution of 0.125 N was used to obtain force measurements at a sampling rate of 8 ms. To compute the commanded velocity in the Z direction, a proportional-derivative force control algorithm was used as follows.

$$v_z = K_p e + K_d \frac{de}{dt} \quad (3)$$

where e is the error between the nominal and measured Z direction force. In this work, K_p and K_d were set to 0.005 and 0.20, respectively. Note that implementation of an integral gain in this work was found to introduce an unacceptable delay because integral wind-up. The peg was determined to be found when the Z force reading was measured to be above -1 N for 20 consecutive measurements. After the peg was found, regular insertion in the Z

direction was conducted until a Z force threshold of -150 N or 10 mm of insertion was passed. **Figure 4B** shows a flow chart representing the insertion and scanning procedure.

QUANTIFYING HUMAN PERFORMANCE

In the case study used in this work, after a failed insertion, the operator manually finished the insertion operation. Thus, the length of insertion by a human operation is used as a metric to define the amount of effort required by personnel in this case study. The manual length of insertion was calculated by computing the difference between the insertion distance by the robot in a failed insertion and the desired insertion distance (10 mm). In addition, the time of manual insertion was used to calculate overall teaming performance. In this work, a single researcher was used to manually test the insertion parameters. Note that the use of a single researcher is sufficient in this case because the study is focused on robot degradation as opposed to cognitive workload and generalizing the results to a human population. In addition, note that human insertion time can be determined from prior literature.²⁸ Thus, manufacturers can also use prior literature as a cost-effective and efficient approach for system integrators to create quantifiable metrics for human-robot collaborative systems.

Results

In this case study, the evaluation of robot degradation on human-robot collaborative systems is presented in the context of the aforementioned metrics. The degradation of the joint 1 angular encoder and joint 2 current sensor were modeled as errors in the forward kinematics and force readings, respectively. Specifically, an error in joint 1 was introduced in the robot position reading in the control system. In addition, errors in the joint 2 current sensor were introduced as an error in the robot force readings using equation (3). For pure insertion, robot degradation errors for the joint 1 encoder and joint 2 current readings were 0.00° , 0.01° , 0.02° , 0.03° , and 0.04° and 0.00 A, 0.25 A, and 0.5 A, respectively. Note that robot manufacturers do not report angular encoder nor current sensor specifications regarding degradation. Thus, the simulated angular degradation is determined by using heuristically determined knowledge. However, Hall Effect sensors are known to report lifetime drift. For instance, the total output error of an Allegro Microsystems ASC71240 Hall Effect sensor is specified to be as high as 5.7%.²⁹ In the case of joint 2 with an average current reading of 5.4 A in the testing configuration, this would correspond to an output error of 0.31 A, which is on the order of the simulated current degradation. For insertion with scanning, robot degradation errors for joint 1 encoder readings were 0.00° , 0.04° , 0.08° , 0.12° , and 0.16° . Note that the robot-force readings were not used for insertion with scanning because of the implementation of the external force/torque sensor, and therefore, current-sensor degradation in joint 2 was not considered. Three repetitions were conducted for each method.

METHOD 1: PURE INSERTION

Figure 5 shows the results of the pure insertion method. Specifically, **figure 5A** shows that the robot with no current degradation (0 A) fails to insert when the joint 1 degradation is 0.04° for this case study. Therefore, the operator must complete the insertion, as shown by the light grey bars. Thus, **figure 5** shows that a fairly minor degradation of 0.04° in a single joint can significantly impact performance. In addition, when the joint 2 current degrades by 0.25 A, the robot fails to insert when the joint 1 angular degradation is 0.03° . However, note that the robot's insertion at 0.03° degradation is larger than at 0.04° . This is because the degradation in the joint 2 current corresponds to a false reading that prematurely stops the insertion process. Thus, the manual insertion effort at 0.03° is less than 0.04° for 0.25-A degradation. When the joint 2 current degrades by 0.50 A, the robot fails to insert even when joint 1 has no degradation. Thus, the manual insertion effort is required for all joint 1 degradation values. Thus, **figure 5A** shows the influence of performance impacts as current sensors degrade. Note that this current degradation can also result in potential safety hazards, especially in poses where the robot forces/torques are particularly sensitive to current, such as the X and Y coordinates of ± 80 mm and -350 mm (**fig. 3**), respectively, where the sensitivity was 129 N/A.

FIG. 5 Results of the pure insertion method corresponding to (A) insertion depth and (B) insertion time.

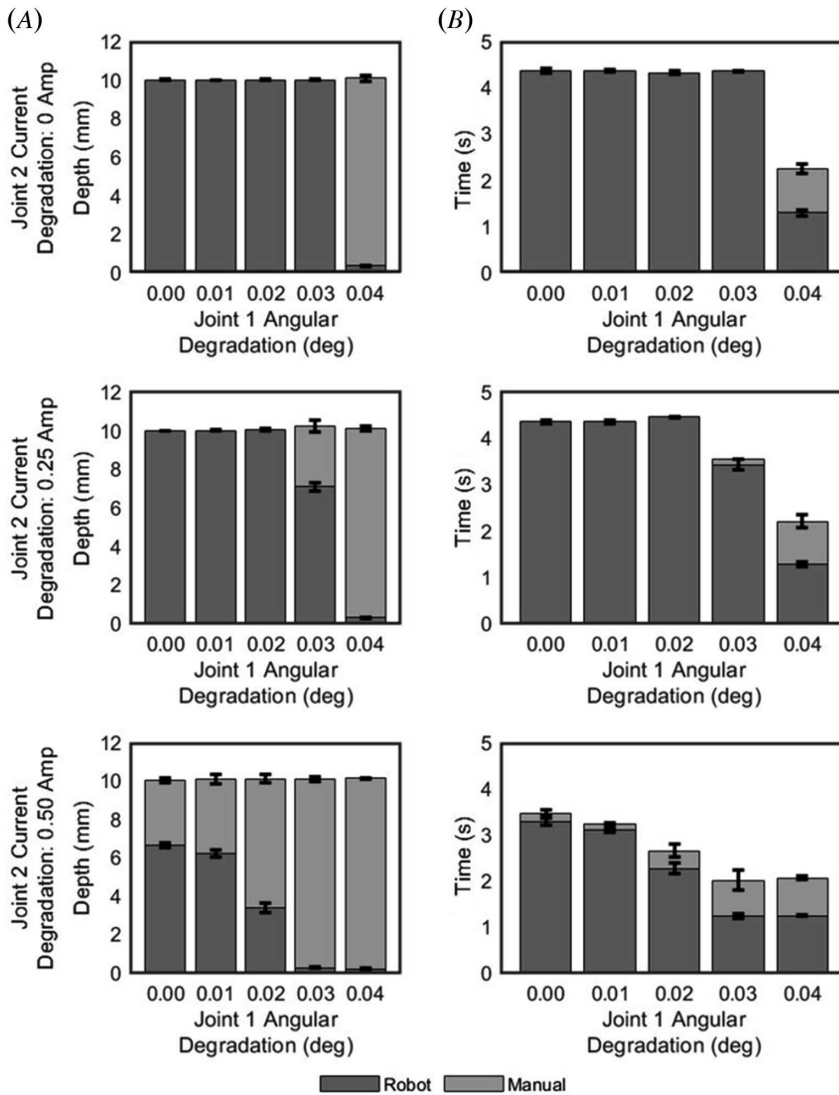


Figure 5B shows the insertion times for the pure insertion method. Interesting to note is that the manual insertion speed appears to be significantly faster than the robot insertion speed. The average manual insertion speed was computed to be 23 ± 9 mm/s, which is much faster than the robot's insertion speed of 3 mm/s. However, increasing the robot's insertion speed to match the manual insertion speed of 23 mm/s could result in potential safety hazards. Note that the insertion speed can increase beyond such a speed after the appropriate safety certification has been conducted before deploying in an industrial environment. Therefore, even though the robot fails to insert, the overall performance time decreases compared to a successful insertion. This is quite normal, as a variety of robot tasks can be done much faster by manufacturing personnel.³⁰ However, intervention by manufacturing personnel results in more human fatigue,³¹ which can impact human performance. Thus, this case study shows that as the robot degrades, the overall insertion time will decrease at the cost of human fatigue.

METHOD 2: INSERTION WITH SCANNING

Figure 6 shows the results of the insertion with the scanning method. Figure 6A shows that the robot fails to insert when the angular degradation reaches 0.12°. This failure value is much larger than with the one with pure insertion (0.04°), thus demonstrating that insertion with scanning is more robust to robot degradation than pure insertion. This result is logical because the scanning phase compensates for inaccuracies in the X-Y position because of degradation in the joint 1 angular position. In addition, it is shown that a joint 1 angular degradation of 0.12° is near the outside of the X-Y scanning area, as some trials exhibited successful insertion while others failed. In addition, figure 6A shows that the X-Y position deviation corresponding to an angular degradation of 0.16° is completely outside the scanning area defined in this work. Theoretically, an implementation of scanning would be able to indefinitely increase the scanning area until the peg is found; however, such an approach will result in a significant loss of time. In addition, 0.16° is expected to be a significant enough degradation that requires external maintenance.

Figure 6B shows the timing results of the insertion with the scanning method. Note that the scanning phase is implemented when the joint 1 angular degradation is greater than 0.04°. Thus, the scanning phase increases the overall successful insertion time from 4.55 s at no degradation to 6.01 s and 12.29 s at 0.08° and 0.12° of angular degradation, respectively. Thus, implementation of the insertion with the scanning method is shown to reduce the effort of the human operator at the cost of a slower insertion time as the robot degrades. Thus, this trade-off that has been shown by the performance metrics as critical for end users to analyze when making their purchasing decisions.

COMPARISON OF OPERATOR WITH PRIOR LITERATURE

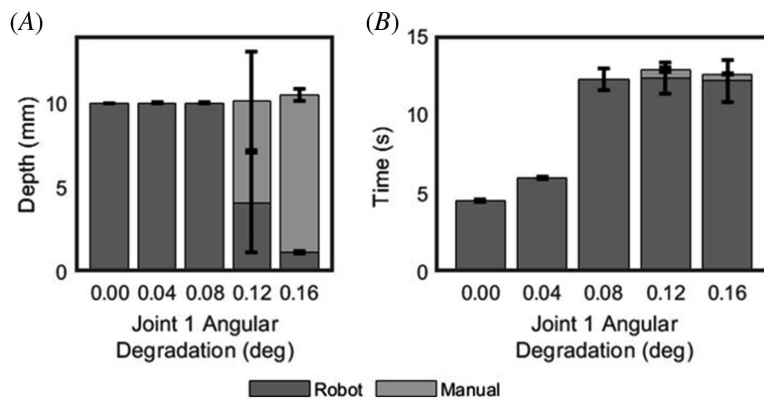
Note that this work focuses on the robot degradation on manufacturing performance in this case study and not the extrapolation of the results to an entire human population, so only one participant was required. However, additional analysis was conducted to evaluate the human insertion time in this study with respect to empirically collected data in prior literature regarding human peg-in-hole assembly times²⁸ where the empirical relation describing the manual insertion time can be calculated as follows:

$$t = -70 \ln \frac{D-d}{d} + 3.7L + 0.75d - 100 \text{ ms} \tag{4}$$

where d , D , and L are the peg diameter, hole diameter, and length of insertion, respectively. Hence, the human insertion time from prior literature can be calculated for all failed insertions and can be statistically compared to the operator values in this work. Therefore, a Wilcoxon signed rank test with a statistical significance of 0.05 was conducted to determine if the median of the population of differences between the data in this work and prior

FIG. 6

Results of the insertion with the scanning method corresponding to (A) insertion depth and (B) insertion time.



literature is zero.³² The test results yield a p -value of 0.12, and therefore, the null hypothesis that the median of the population of differences is zero cannot be rejected.

Conclusions

This paper examines the influence of robot degradation on human-robot collaborative systems in manufacturing applications. Teaming performance metrics are described in the context of robot degradation. These metrics are applied to a peg-in-hole case study where manual intervention is required if the robot fails in its initial attempt to insert an end effector over a peg. Two robot methods involving pure insertion and insertion with scanning were analyzed under the influences of angular encoder and current sensor degradation. The results show that the pure insertion method required more manual intervention as the robot degraded and failed to conduct full insertion. In addition, the insertion with the scanning method was more robust to robot degradation, and therefore required less manual intervention, at the cost of insertion time. Note that this work could have used prior literature to evaluate the influence of manual intervention from a manufacturing-performance perspective. Hence, robot manufacturers and system integrators that wish to evaluate the performance of human-robot collaborative systems in general do not require human subjects for quantifying their metrics. Thus, metrics for quantifying the performance of such systems can be easily adopted for end users to make informed process-planning decisions.

However, note that more complex manufacturing tasks require methods that combine simplistic tasks for quantifying performance. Hence, such methods are subject to future work. In addition, the case study used in this work involves sequential operations where the robot conducts a task and the operator may conduct a subsequent task. Thus, another subject of future work involves studying the influence of robot degradation on active collaborative systems including load-sharing applications. Finally, though expected to be a minor impact on manufacturing performance, social aspects, including cognitive load and trust, can be studied as future work.

DISCLAIMER

Certain commercial equipment, instruments, or materials are identified in this paper in order to specify the experimental procedure adequately. Such identification is not intended to imply recommendation or endorsement by NIST, nor is it intended to imply that the materials or equipment identified are necessarily the best available for the purpose.

ACKNOWLEDGMENTS

This work was funded by the National Institute of Standards and Technology and the National Research Council Research Associateship Program.

References

1. H. S. Kang, J. Y. Lee, S. Choi, H. Kim, J. H. Park, J. Y. Son, B. H. Kim, and S. Do Noh, "Smart Manufacturing: Past Research, Present Findings, and Future Directions," *International Journal of Precision Engineering and Manufacturing-Green Technology* 3, no. 1 (January 2016): 111–128, <https://doi.org/10.1007/s40684-016-0015-5>
2. L. D. Evjemo, T. Gjerstad, E. I. Grøtli, and G. Sziebig, "Trends in Smart Manufacturing: Role of Humans and Industrial Robots in Smart Factories," *Current Robotics Reports* 1, no. 2 (April 2020): 35–41, <https://doi.org/10.1007/s43154-020-00006-5>
3. P. Tsarouchi, S. Makris, and G. Chryssolouris, "Human–Robot Interaction Review and Challenges on Task Planning and Programming," *International Journal of Computer Integrated Manufacturing* 29, no. 8 (February 2016): 916–931, <https://doi.org/10.1080/0951192X.2015.1130251>
4. E. Matheson, R. Minto, E. G. G. Zampieri, M. Faccio, and G. Rosati, "Human–Robot Collaboration in Manufacturing Applications: A Review," *Robotics* 8, no. 4 (December 2019): 100, <https://doi.org/10.3390/robotics8040100>
5. J. A. Marvel, S. Bagchi, M. Zimmerman, and B. Antonishek, "Towards Effective Interface Designs for Collaborative HRI in Manufacturing: Metrics and Measures," *ACM Transactions on Human-Robot Interaction* 9, no. 4 (October 2020): 1–55, <https://doi.org/10.1145/3385009>
6. S. Singer and D. Akin, "A Survey of Quantitative Team Performance Metrics for Human-Robot Collaboration," in *41st International Conference on Environmental Systems* (Reston, VA: American Institute of Aeronautics and Astronautics, 2011), 1–19, <https://doi.org/10.2514/6.2011-5248>

7. J. A. Marvel, J. Falco, and I. Marstio, "Characterizing Task-Based Human-Robot Collaboration Safety in Manufacturing," *IEEE Transactions on Systems, Man, and Cybernetics: Systems* 45, no. 2 (July 2014): 260–275, <https://doi.org/10.1109/TSMC.2014.2337275>
8. A. M. Zanchettin, N. M. Ceriani, P. Rocco, H. Ding, and B. Matthias, "Safety in Human-Robot Collaborative Manufacturing Environments: Metrics and Control," *IEEE Transactions on Automation Science and Engineering* 13, no. 2 (April 2015): 882–893, <https://doi.org/10.1109/TASE.2015.2412256>
9. P. Gustavsson, M. Holm, A. Syberfeldt, and L. Wang, "Human-Robot Collaboration – towards New Metrics for Selection of Communication Technologies," *Procedia CIRP* 72 (January 2018): 123–128, <https://doi.org/10.1016/j.procir.2018.03.156>
10. A. Steinfeld, T. Fong, D. Kaber, M. Lewis, J. Scholtz, A. Schultz, and M. Goodrich, "Common Metrics for Human-Robot Interaction," in *Proceedings of the First ACM SIGCHI/SIGART Conference on Human-Robot Interaction* (New York: Association for Computing Machinery, 2006), 33–40, <https://doi.org/10.1145/1121241.1121249>
11. K. E. Schaefer, J. Y. C. Chen, J. L. Szalma, and P. A. Hancock, "A Meta-Analysis of Factors Influencing the Development of Trust in Automation: Implications for Understanding Autonomy in Future Systems," *Human Factors* 58 no. 3 (March 2016): 377–400, <https://doi.org/10.1177/00187208166634228>
12. G. Qiao and B. A. Weiss, "Accuracy Degradation Analysis for Industrial Robot Systems," in *ASME 2017 12th International Manufacturing Science and Engineering Conference* (New York: American Society of Mechanical Engineers, 2017), V003T04A006, <https://doi.org/10.1115/MSEC2017-2782>
13. U. Izagirre, I. Andonegui, L. Eciolaza, and U. Zurutuza, "Towards Manufacturing Robotics Accuracy Degradation Assessment: A Vision-Based Data-Driven Implementation," *Robot and Computer-Integrated Manufacturing* 67 (February 2021): 102029, <https://doi.org/10.1016/j.rcim.2020.102029>
14. R. N. A. Algburi and H. Gao, "Health Assessment and Fault Detection System for an Industrial Robot Using the Rotary Encoder Signal," *Energies* 12, no. 14 (July 2019): 2816, <https://doi.org/10.3390/en12142816>
15. B. A. Weiss and J. Kaplan, "Assessment of a Novel Position Verification Sensor to Identify and Isolate Robot Workcell Health Degradation," *Journal of Manufacturing Science and Engineering* 143, no. 4 (April 2021): 041008, <https://doi.org/10.1115/1.4048446>
16. S. Moon and G. S. Virk, "Survey on ISO Standards for Industrial and Service Robots," in *ICCAS-SICE* (Tokyo: Society of Instrument and Control Engineers, 2009), 1878–1881.
17. J. Fryman and B. Matthias, "Safety of Industrial Robots: From Conventional to Collaborative Applications," in *ROBOTIK 2012; Seventh German Conference on Robotics* (Frankfurt, Germany: VDE Association for Electrical, Electronic and Information Technologies, 2012), 1–5.
18. A. Klinger and B. A. Weiss, "Examining Workcell Kinematic Chains to Identify Sources of Positioning Degradation" (paper presentation, Annual Conference of the Prognostics and Health Management Society 2018, Philadelphia, PA, September 24–27, 2018), http://web.archive.org/web/20200322170540/https://tsapps.nist.gov/publication/get_pdf.cfm?pub_id=926386
19. P. Aivaliotis, S. Aivaliotis, C. Gkournelos, K. Kokkalis, G. Michalos, and S. Makris, "Power and Force Limiting on Industrial Robots for Human-Robot Collaboration," *Robotics and Computer-Integrated Manufacturing* 59 (October 2019): 346–360, <https://doi.org/10.1016/j.rcim.2019.05.001>
20. F.-F. Xi, L. Yu, and X.-W. Tu, "Framework on Robotic Percussive Riveting for Aircraft Assembly Automation," *Advances in Manufacturing* 1, no. 2 (April 2013): 112–122, <https://doi.org/10.1007/s40436-013-0014-5>
21. J. Mahler, M. Matl, X. Liu, A. Li, D. Gealy, and K. Goldberg, "Dex-Net 3.0: Computing Robust Robot Vacuum Suction Grasp Targets in Point Clouds Using a New Analytic Model and Deep Learning," in *2018 IEEE International Conference on Robotics and Automation (ICRA)* (Piscataway, NJ: Institute of Electrical and Electronics Engineers, 2018), 5620–5627, <https://doi.org/10.1109/ICRA.2018.8460887>
22. D. E. Orin and W. W. Schrader, "Efficient Computation of the Jacobian for Robot Manipulators," *The International Journal of Robotics Research* 3, no. 4 (December 1984): 66–75, <https://doi.org/10.1177/027836498400300404>
23. M. W. Spong, S. Hutchinson, and M. Vidyasagar, *Robot Modeling and Control* (Hoboken, NJ: Wiley, 2005).
24. G. Wu, X. Liu, Z. Liang, Y. Wang, and X. Wang, "Research on Diameter Tolerance of Transmission Shaft Based on Interval Analysis," *Journal of Failure Analysis and Prevention* 19, no. 1 (January 2019): 154–160, <https://doi.org/10.1007/s11668-019-00584-3>
25. J. Wang, H. Zhang, and T. Fuhlbrigge, "Improving Machining Accuracy with Robot Deformation Compensation," in *2009 IEEE/RSJ International Conference on Intelligent Robots and Systems* (Piscataway, NJ: Institute of Electrical and Electronics Engineers, 2009), 3826–3831, <https://doi.org/10.1109/IROS.2009.5353988>
26. L. Biagiotti and C. Melchiorri, *Trajectory Planning for Automatic Machines and Robots* (Berlin: Springer, 2008), <https://doi.org/10.1007/978-3-540-85629-0>
27. J. A. Marvel, R. Bostelman, and J. Falco, "Multi-robot Assembly Strategies and Metrics," *ACM Computing Surveys* 51, no. 1 (April 2018): 1–32, <https://doi.org/10.1145/3150225>
28. G. Boothroyd, P. Dewhurst, and W. A. Knight, *Product Design for Manufacture and Assembly*, 3rd ed. (Boca Raton, FL: CRC Press, 2011).
29. Allegro Microsystems, "ACS71240: Automotive-Grade, Galvanically Isolated Current Sensor IC with Common-Mode Field Rejection and Overcurrent Detection in Small Footprint Low-Profile Packages," Allegro Microsystems, 2020,

- <http://web.archive.org/web/20210729140342/https://www.allegromicro.com/en/products/sense/current-sensor-ics/zero-to-fifty-amp-integrated-conductor-sensor-ics/acs71240>
30. B. D. Argall, S. Chernova, M. Veloso, and B. Browning, "A Survey of Robot Learning from Demonstration," *Robotics and Autonomous Systems* 57, no. 5 (May 2009): 469–483, <https://doi.org/10.1016/j.robot.2008.10.024>
 31. L. Peternel, N. Tsagarakis, D. Caldwell, and A. Ajoudani, "Adaptation of Robot Physical Behaviour to Human Fatigue in Human-Robot Co-manipulation," in *2016 IEEE-RAS 16th International Conference on Humanoid Robots (Humanoids)* (Piscataway, NJ: Institute of Electrical and Electronics Engineers), 489–494, <https://doi.org/10.1109/HUMANOIDS.2016.7803320>
 32. R. F. Woolson, "Wilcoxon Signed-Rank Test," in *Wiley Encyclopedia of Clinical Trials* (Hoboken, NJ: Wiley, 2008), 1–3, <https://doi.org/10.1002/9780471462422.eoct979>